LETTER

doi:10.1038/nature10726

Topoisomerase inhibitors unsilence the dormant allele of *Ube3a* in neurons

Hsien-Sung Huang[1]*, John A. Allen[2]*, Angela M. Mabb[1], Ian F. King[1], Jayalakshmi Miriyala[1], Bonnie Taylor-Blake[1], Noah Sciaky[2], J. Walter Dutton Jr[1], Hyeong-Min Lee[2], Xin Chen[3], Jian Jin[3], Arlene S. Bridges[4], Mark J. Zylka[1,5,6], Bryan L. Roth[2,5,6,7,8] & Benjamin D. Philpot[1,5,6]

Angelman syndrome is a severe neurodevelopmental disorder caused by deletion or mutation of the maternal allele of the ubiquitin protein ligase E3A (*UBE3A*)[1–3]. In neurons, the paternal allele of *UBE3A* is intact but epigenetically silenced[4–6], raising the possibility that Angelman syndrome could be treated by activating this silenced allele to restore functional UBE3A protein[7,8]. Using an unbiased, high-content screen in primary cortical neurons from mice, we identify twelve topoisomerase I inhibitors and four topoisomerase II inhibitors that unsilence the paternal *Ube3a* allele. These drugs included topotecan, irinotecan, etoposide and dexrazoxane (ICRF-187). At nanomolar concentrations, topotecan upregulated catalytically active UBE3A in neurons from maternal *Ube3a*-null mice. Topotecan concomitantly downregulated expression of the *Ube3a* antisense transcript that overlaps the paternal copy of *Ube3a*[9–11]. These results indicate that topotecan unsilences *Ube3a* in *cis* by reducing transcription of an imprinted antisense RNA. When administered *in vivo*, topotecan unsilenced the paternal *Ube3a* allele in several regions of the nervous system, including neurons in the hippocampus, neocortex, striatum, cerebellum and spinal cord. Paternal expression of *Ube3a* remained elevated in a subset of spinal cord neurons for at least 12 weeks after cessation of topotecan treatment, indicating that transient topoisomerase inhibition can have enduring effects on gene expression. Although potential off-target effects remain to be investigated, our findings suggest a therapeutic strategy for reactivating the functional but dormant allele of *Ube3a* in patients with Angelman syndrome.

No effective therapies exist for Angelman syndrome—an imprinting disorder caused by mutations or deletions in the maternal allele of *UBE3A*[1–3]. *Ube3a* is biallelically expressed in most tissues of the body; however, in rodents and humans, most neurons express *Ube3a* only from the maternally-inherited allele[4,12–14]. This unique epigenetic pattern of regulation suggested that it might be possible to unsilence the dormant paternal *Ube3a* allele in neurons[7,8].

To test this possibility, we developed a 384-well high-content screen using primary mouse cortical neurons from *Ube3a*–yellow fluorescent protein (*Ube3a–YFP*) knock-in mice[15], and searched for drug-like molecules that could unsilence the paternal *Ube3a–YFP* allele (Fig. 1a). This screen was based on our observation that the imprinting of *Ube3a–YFP* was maintained *in vitro* in cultured embryonic cortical neurons. Notably, *Ube3a–YFP* expression was undetectable (silenced) in cultured neurons when *Ube3a–YFP* was paternally inherited ($Ube3a^{m+/pYFP}$), but was expressed when *Ube3a–YFP* was maternally inherited ($Ube3a^{mYFP/p+}$) (Fig. 1b), with expression increasing from 4 to 10 days *in vitro* (DIV) (Fig. 1c). This significant difference between maternal and paternal UBE3A–YFP protein levels provided a large screening window and a Z'-factor score of 0.58 (determined by statistically comparing antibody-enhanced fluorescence intensities and variations between maternal and paternal UBE3A–YFP signals at DIV10), making our high-content platform suitable for unbiased screening.

To perform the screen, we cultured $Ube3a^{m+/pYFP}$ neurons for 7 days and then treated these neurons with compounds (10 μM for 72 h) from several small-molecule libraries (Fig. 1d and Supplementary Fig. 1). In total, we screened 2,306 small molecules in quadruplicate, normalizing values to vehicle-treatment (0.2% dimethyl sulphoxide (DMSO)) (for full methods see Supplementary Methods; for list of all compounds tested see Supplementary Table 1). Although methylation and other epigenetic marks are thought to control imprinting of *Ube3a*[9,16–18], to our surprise, none of the commonly used compounds that target the epigenome, including chromatin-remodelling drugs and DNA methyltransferase inhibitors, unsilenced the paternal *Ube3a–YFP* allele. A number of compounds were identified as false positives (grey compounds in Fig. 1d) due to their intrinsic fluorescence (Supplementary Fig. 2). Our initial screen identified one compound—irinotecan, an FDA-approved topoisomerase type I inhibitor. Irinotecan lacked intrinsic fluorescence and upregulated UBE3A–YFP fluorescence (Fig. 1d, e and Supplementary Fig. 3). Irinotecan (10 μM) also upregulated paternal UBE3A–YFP protein (Fig. 1f) and endogenous UBE3A protein (Fig. 1g) in neuronal cultures from $Ube3a^{m+/pYFP}$ and $Ube3a^{m-/p+}$ mice (Angelman syndrome model mice[13]), respectively.

Many topoisomerase I inhibitors, including irinotecan and the related FDA-approved drug topotecan, are derived from the natural product camptothecin (CPT)[19]. To explore structure activity relationships, we tested CPT analogues and other topoisomerase inhibitors (Fig. 2a and Supplementary Figs 4–10). The analogues we tested all lack inherent fluorescence (Supplementary Fig. 3). We found that irinotecan and topotecan upregulated paternal UBE3A–YFP in a dose- and time-dependent manner in cultured neurons, with topotecan being 20 times more potent than irinotecan (Fig. 2a, b and Supplementary Fig. 11). In contrast, an inactive analogue of CPT (lactam E ring-CPT) that does not inhibit topoisomerases[20] failed to unsilence the paternal *Ube3a–YFP* allele (Fig. 2a and Supplementary Fig. 4). Ten additional topoisomerase I inhibitors unsilenced *Ube3a–YFP* in a dose-dependent manner, including CPT analogues and structurally distinct indenoisoquinolines (Table 1 and Supplementary Figs 4–7). Furthermore, four structurally distinct topoisomerase II inhibitors (etoposide, dexrazoxane, ICRF-193 and amsacrine) also unsilenced the paternal *Ube3a–YFP* allele (Table 1 and Supplementary Figs 8–10). Thus, our data with 16 topoisomerase inhibitors and one inactive analogue strongly suggest that inhibition of topoisomerase I or II can unsilence the paternal *Ube3a* allele.

[1]Department of Cell and Molecular Physiology, University of North Carolina School of Medicine, Chapel Hill, North Carolina 27599, USA. [2]Department of Pharmacology, University of North Carolina School of Medicine, Chapel Hill, North Carolina 27599, USA. [3]Center for Integrative Chemical Biology and Drug Discovery, Division of Chemical Biology and Medicinal Chemistry, University of North Carolina Eshelman School of Pharmacy, Chapel Hill, North Carolina 27599, USA. [4]Department of Pathology and Laboratory Medicine, University of North Carolina School of Medicine, Chapel Hill, North Carolina 27599, USA. [5]Carolina Institute for Developmental Disabilities, University of North Carolina, Chapel Hill, North Carolina 27599, USA. [6]University of North Carolina Neuroscience Center, Chapel Hill, North Carolina 27599, USA. [7]Division of Chemical Biology and Medicinal Chemistry, University of North Carolina Eshelman School of Pharmacy, Chapel Hill, North Carolina 27599, USA. [8]National Institute of Mental Health, Psychoactive Drug Screening Program, Department of Pharmacology, University of North Carolina School of Medicine, Chapel Hill, North Carolina 27599, USA.
*These authors contributed equally to this work.

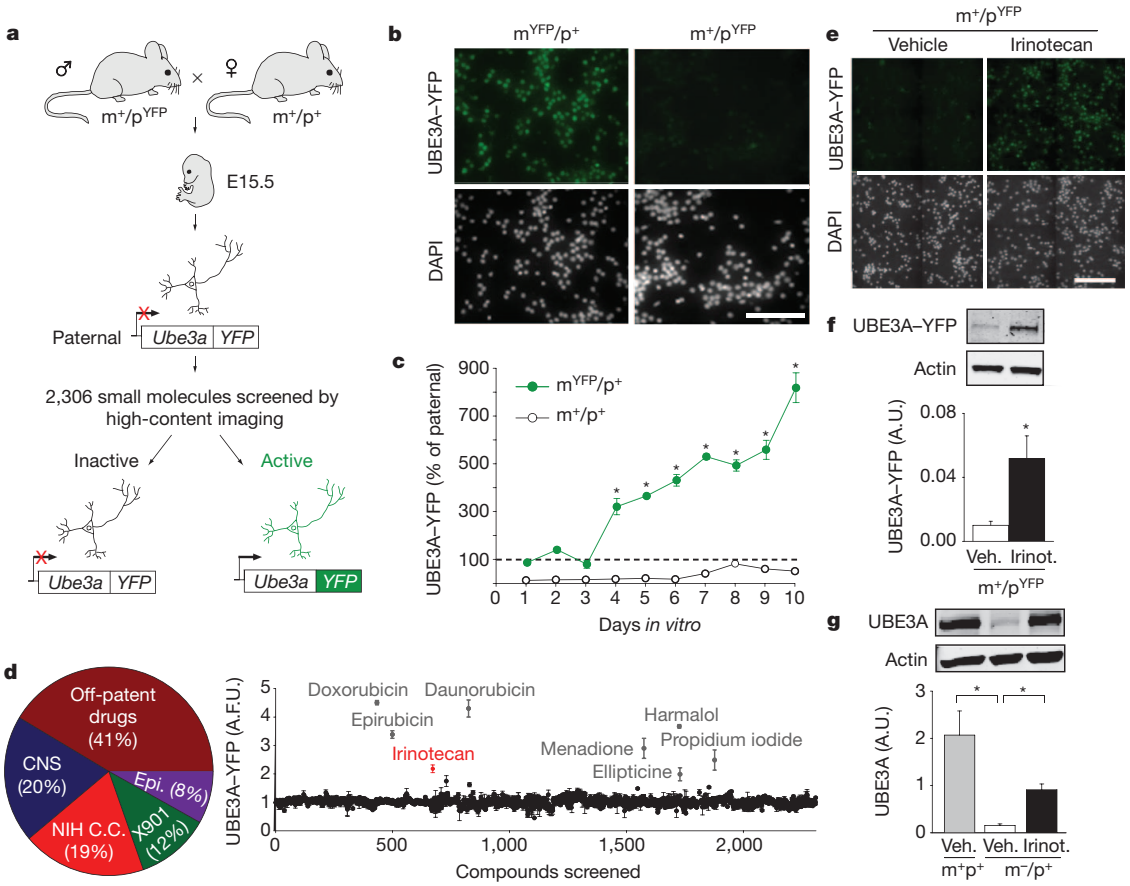

Figure 1 | A small-molecule screen identifies a topoisomerase inhibitor that unsilences the paternal allele of *Ube3a* in neurons. **a**, High-content screen flowchart. Embryonic day 15.5 (E15.5) cortical neurons with a paternally inherited *Ube3a–YFP* allele were cultured in 384-well plates and treated with small molecules from DIV7–DIV10. Active compounds that unsilence the paternal *Ube3a–YFP* allele were detected with antibody-enhanced fluorescence and high-content imaging. **b**, High-content imaging of DIV7 neurons that inherited *Ube3a–YFP* maternally (m^{YFP}/p^{+}) or paternally (m^{+}/p^{YFP}). Nuclei were stained with 4′,6-diamidino-2-phenylindole (DAPI). Scale bar, 50 μm. **c**, Mean ± s.e.m. levels of UBE3A–YFP fluorescence in neurons cultured from maternal *Ube3a–YFP* (m^{YFP}/p^{+}) or wild-type (m^{+}/p^{+}) mice, normalized to levels in age-matched neurons cultured from paternal *Ube3a–YFP* mice (m^{+}/p^{YFP}). Two-way analysis of variance (ANOVA) revealed main effects of genotype, duration and a genotype–duration interaction ($P < 0.001$); Bonferroni post hoc test examined comparisons between maternal and paternal *Ube3a–YFP* mice from DIV4 to DIV10, $^{*}P < 0.001$; $n = 2$–6 culture wells per day. **d**, Pie chart depicting categories of the 2,306 screened compounds and graph summarizing presumptive UBE3A–YFP in arbitrary fluorescence units (A.F.U.) after small molecule treatments. CNS, central nervous system selective small molecule library; Epi., epigenetic small molecule library; NIH C.C., NIH Clinical Collection; X901, NIMH X-901 small molecule library. Small molecules that were subsequently found to be autofluorescent (Supplementary Fig. 2) are depicted in grey. The initial screen identified one active compound, irinotecan (red). **e**, High-magnification view of wells treated with vehicle (0.2% DMSO) or 10 μM irinotecan for 72 h. Neuron density and health is similar in vehicle- and irinotecan-treated cells as evidenced by counterstaining with the nuclear marker DAPI. Scale bar, 100 μm. **f**, **g**, Western blots of cultured cortical neurons probed with GFP or UBE3A antibodies, respectively, with or without irinotecan (10 μM for 72 h). Irinot., irinotecan; Veh., vehicle. **f**, $^{*}P < 0.05$; two-tailed *t*-test, $n = 3$ per group. **g**, $^{*}P < 0.001$, one-way ANOVA with Bonferroni post hoc, $n = 7$–8 per group. All data are presented as means ± s.e.m.

We focused our remaining studies on the topoisomerase I inhibitor topotecan because it is approved for use in humans, it unsilenced *Ube3a* in the low nanomolar range, and topotecan (300 nM, 72 h) restored UBE3A protein to wild-type levels in cultured neurons from $Ube3a^{m-/p+}$ mice (Fig. 2c).

Many topoisomerase inhibitors, including topotecan, covalently link topoisomerases to DNA, forming stable DNA–enzyme complexes that are separable from free topoisomerase enzymes[19]. Because topotecan inhibits topoisomerase I (TOP1) and *Top1* is expressed at high levels in the developing and adult brain[19,21], we focused our subsequent analysis on this enzyme. We found that topotecan (300 nM, 72 h) significantly reduced the amount of free TOP1 (Fig. 2d) in cultured neurons, indicating that topotecan engages its known molecular target at doses that unsilence the paternal *Ube3a* allele.

UBE3A is a HECT (homology to E6 carboxyl terminus) domain E3 ligase that forms a thioester-ubiquitin intermediate in the presence of E1 and E2 enzymes[22]. This thioester-ubiquitin intermediate is required for HECT domain E3 ligases to mono- and polyubiquitinate their substrates[23]. Interestingly, we noticed that topotecan (300 nM, 72 h) upregulated UBE3A protein in $Ube3a^{m-/p+}$ cultures along with a higher molecular weight form (resolved after running gels for longer times; Fig. 2e). This high molecular weight band was also seen in wild-type ($Ube3a^{m+/p+}$) cultures and was lost upon addition of the reducing agent dithiothreitol (DTT) (Fig. 2e). These data indicate that the unsilenced paternal copy of UBE3A is catalytically active and competent to form a thioester-ubiquitin intermediate, just like wild-type, maternal-derived UBE3A.

To demonstrate further that UBE3A was catalytically active, we immunoprecipitated UBE3A from cultured wild-type and $Ube3a^{m-/p+}$ neurons (with or without topotecan), then tested these samples using a gel-mobility shift assay in the presence or absence of the ubiquitin E2 UBCH7 (ref. 24). Both wild-type (maternal-derived) and topotecan-unsilenced (paternal-derived) UBE3A underwent mobility shifts in the presence of UBCH7 plus free ubiquitin that were abolished by addition of DTT (Fig. 2f). This observation indicates the mobility shift was due to addition of covalent ubiquitin, and demonstrates that topotecan can upregulate a functional UBE3A enzyme.

Table 1 | Efficacies and potencies of topoisomerase inhibitors for unsilencing the paternal allele of *Ube3a–YFP* in cultured neurons

Compound	Potency (half-maximum effective concentration EC_{50}, nM)	Efficacy E_{max} (fold over vehicle)
Camptothecin derivatives		
7-ethyl-camptothecin (7-ethyl-CPT)	7.2 ± 2.3	1.70 ± 0.04
7-ethyl-10-hydroxy-CPT	11 ± 3.2	1.99 ± 0.06
10-hydroxy-CPT	14 ± 5.7	1.82 ± 0.08
Belotecan (CKD602)	19 ± 4.4	1.88 ± 0.05
Camptothecin (CPT)	21 ± 3.8	2.11 ± 0.05
Topotecan*	54 ± 3.4	2.25 ± 0.05
Rubitecan (9-nitro-CPT)	62 ± 18	2.09 ± 0.09
Irinotecan*	994 ± 13	2.17 ± 0.05
Silatecan (DB67)	2,244 ± 171	1.65 ± 0.05
Lactam E ring-CPT (inactive)	inactive	inactive
Indenoisoquinoline derivatives		
NSC725776	10 ± 1.6	1.76 ± 0.03
NSC706744	11 ± 3.2	1.84 ± 0.07
NSC724998	14 ± 2.2	1.69 ± 0.03
Podophyllotoxin derivative		
Etoposide*	1,600 ± 980	1.68 ± 0.04
Bis-dioxopiperazine derivatives		
ICRF-193	205 ± 70	2.21 ± 0.09
Dexrazoxane (ICRF-187)*	20,470 ± 1,450	1.82 ± 0.05
Aminoacridine derivative		
Amsacrine	27 ± 5.2	1.74 ± 0.06

* FDA-approved compounds.

Ube3a is repressed in *cis* by a large antisense transcript (*Ube3a–ATS*) that overlaps the paternal allele of *Ube3a* (Fig. 2g)[9–11]. *Ube3a–ATS* is expressed exclusively from the paternal allele as a result of allele-specific methylation of an imprinting centre that overlaps the *Ube3a–ATS* and *Snurf/Snrpn* transcription start site[25]. We next sought to determine if topotecan regulated *Ube3a* expression through changes in *Ube3a–ATS* expression or altered methylation at the imprinting centre. We found that topotecan upregulated expression of *Ube3a* in cultured neurons from $Ube3a^{m-/p+}$ mice while concomitantly down-regulating expression of *Ube3a–ATS* and *Snurf/Snrpn* (Fig. 2h). However, topotecan did not alter methylation at the imprinting centre (Fig. 2i and Supplementary Fig. 12). Taken together, these data indicate that topotecan unsilences paternal *Ube3a* by reducing transcription of a regulatory antisense RNA without appreciably affecting genomic methylation at the imprinting centre.

We then sought to determine if topotecan could unsilence the paternal *Ube3a* allele *in vivo*. We first identified a dose that was well tolerated, meaning there were no significant decreases in body weight between the beginning and end of the drug treatments (Supplementary Fig. 13). We then administered topotecan (3.74 $\mu g\,h^{-1}$) unilaterally into the lateral ventricle of $Ube3a^{m+/pYFP}$ or $Ube3a^{m-/p+}$ mice by intracerebroventricular (i.c.v.) infusion for 2 weeks and then killed the mice

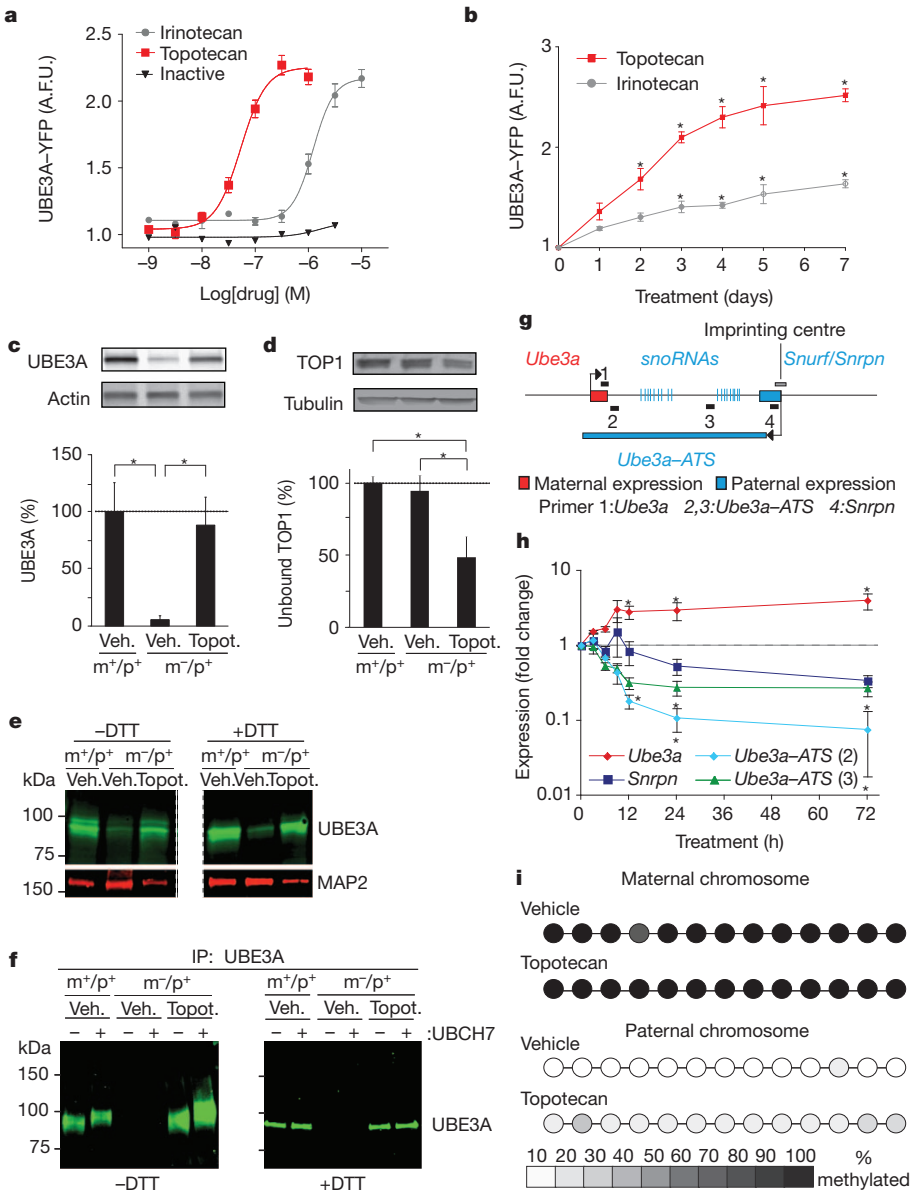

Figure 2 | Topotecan unsilences the paternal allele of *Ube3a* and the unsilenced protein is catalytically active. **a**, Dose–response curves for unsilencing paternal *Ube3a–YFP*. Inactive, lactam E ring-camptothecin. $n = 4$ per data point. **b**, UBE3A–YFP levels in neurons from $Ube3a^{m+/pYFP}$ mice increase with duration of topotecan (300 nM) or irinotecan (1 μM) treatment. $^*P < 0.05$, one-way ANOVA with Bonferroni post hoc tests relative to day zero, $n = 4$–8 per group. A.F.U., arbitrary fluorescence units. **c**, Western blots and quantification of UBE3A and the loading control β-actin. $^*P < 0.05$, one-way ANOVA with Bonferroni post hoc tests, $n = 4$ per group. Topot., topotecan. **d**, Quantification of unbound TOP1 and representative western blots. β-tubulin was used as a loading control. One-way ANOVA with Bonferroni post hoc tests, $^*P < 0.05$; $n = 3$ per group. **e**, Western blot from vehicle- and topotecan-treated neurons from wild-type (m^+/p^+) and maternal *Ube3a*-deficient (m^-/p^+) mice. **f**, Western blots examining UBE3A ubiquitin-thioester formation following immunoprecipitation with an anti-UBE3A antibody and *in vitro* ubiquitination in the presence or absence of the ubiquitin-conjugating enzyme (E2), UBCH7. All data are presented as means ± s.e.m. **g**, Schematic demonstrating location of four primer sets used to probe mRNA expression shown in **h**. **h**, Normalized mRNA levels in cultured $Ube3a^{m-/p+}$ neurons after vehicle or 300 nM topotecan treatment. Expression is given as a ratio of expression in drug-treated cells to vehicle-treated cells, normalized to the housekeeping gene *RPL22*. $^*P < 0.05$ compared to 0 h, Kruskal–Wallis one-way ANOVA followed by post hoc tests, $n = 4$–5 cultures per data point. **i**, Schematic summarizing methylation status of the *Snrpn* promoter region on the maternal and paternal chromosome following treatment with vehicle or 300 nM topotecan (see complete data set in Supplementary Fig. 12). Average methylation status is indicated using a greyscale.

either immediately or 5 h after drug cessation. Strikingly, topotecan unsilenced paternal *Ube3a* in the hippocampus, striatum and cerebral cortex of the infused hemisphere, but had only a modest effect on the contralateral (non-infused) hemisphere with no effect in the cerebellum (Fig. 3a–e and Supplementary Figs 14–15). Pharmacokinetic analyses demonstrated that a significant amount of topotecan was detectable in the infused hemisphere immediately after treatment, whereas low levels were present in the contralateral (non-infused) hemisphere and in cerebellum (Fig. 3a and Supplementary Fig. 14). However, a higher dose of topotecan (21.6 $\mu g\,h^{-1}$ for 5 days) did unsilence the paternal allele of *Ube3a* in Purkinje neurons of the cerebellum (Supplementary Fig. 16). No significant difference in topotecan levels was detected in blood between drug- and vehicle-treated mice (data not shown). Topotecan concentrations significantly declined five hours after cessation of i.c.v. drug delivery (Fig. 3a), indicating that topotecan does not persist and is rapidly removed/metabolized in the brain. Taken together, these pharmacokinetic and pharmacodynamic data indicate that the degree to which topotecan unsilences the paternal *Ube3a* allele is directly correlated with drug concentrations in the brain. Moreover, our data indicate topotecan has the potential to unsilence the paternal *Ube3a* allele throughout the nervous system.

Genomic imprinting is thought to be established only during prescribed germline and embryonic periods of development and imprinted genes typically remain epigenetically regulated throughout life[26]. Thus, we next sought to determine if topotecan had transient or long-lasting effects on paternal *Ube3a* expression. To test this possibility, we turned to an intrathecal (i.t.) delivery protocol (Fig. 3f) because topotecan (Fig. 3g) and irinotecan (not shown) unsilenced paternal *Ube3a* in a sparse population of lumbar spinal neurons, allowing us to quantify all UBE3A–YFP-positive neurons. Moreover, i.t. delivery has been used to deliver topotecan to the brain in humans[27]. We found that topotecan (50 nmol in 5 µl; i.t. once daily, for 10 out of 14 days) was well tolerated (Supplementary Fig. 13) and significantly increased the number of paternal UBE3A–YFP-positive cells in the lumbar spinal cord of mice (Fig. 3g, h and Supplementary Fig. 17a). The vast majority (>93%) of these UBE3A–YFP-positive cells were $NeuN^+$ neurons (Supplementary Fig. 17a, b), indicating topotecan primarily unsilences *Ube3a* in neurons *in vivo*. Moreover, the unsilenced paternal UBE3A–YFP protein was expressed at levels comparable to maternal UBE3A–YFP controls (Supplementary Fig. 17c). Remarkably, the number of UBE3A–YFP-positive spinal cord neurons remained elevated 12 weeks after cessation of drug treatment (Fig. 3g, h), much longer than the elimination of topotecan from tissue (Fig. 3a). These results indicate that topotecan can enduringly unsilence paternal *Ube3a* in a subset of spinal neurons and indicate that a single course of drug treatment has the capacity to permanently modify expression of *Ube3a*.

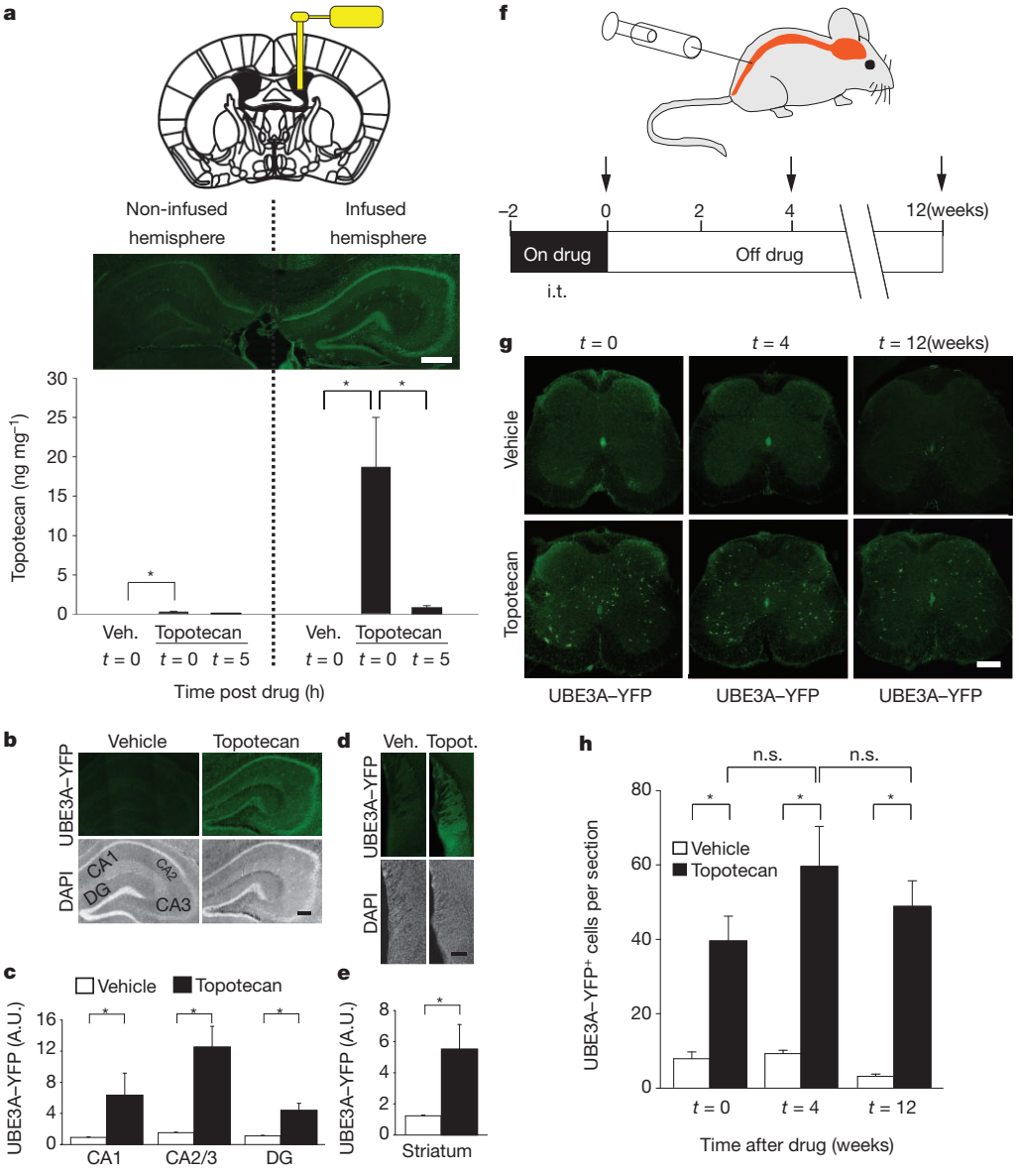

Figure 3 | Topotecan enduringly unsilences the paternal allele of *Ube3a in vivo*. **a**, Unilateral delivery of topotecan (i.c.v.) using a mini-osmotic pump into the lateral ventricle of $Ube3a^{m+/pYFP}$ mice *in vivo*. Two weeks of topotecan infusion (3.74 $\mu g\,h^{-1}$) unsilenced the paternal *Ube3a–YFP* allele in the hippocampus of the infused hemisphere near the site of drug delivery, while only modestly unsilencing *Ube3a–YFP* in the contralateral (non-infused) hemisphere. Scale bar, 500 µm. Pharmacokinetic analyses measuring topotecan levels in the infused and non-infused hemisphere immediately ($t = 0$) or 5 hours ($t = 5$) after cessation of drug delivery. $^*P < 0.05$, one-way ANOVA with Bonferroni post hoc test, $n = 5$–9 per group. **b**, Representative sections and **c**, quantification of optical intensity of UBE3A–YFP in hippocampal regions (CA1, CA2/3 and dentate gyrus, DG) of the topotecan-infused hemisphere or the hemisphere of vehicle-treated mice. $^*P < 0.05$, Mann–Whitney rank sum test, $n = 5$ per group. **d**, Representative sections and **e**, quantification of paternal UBE3A–YFP in the striatum following i.c.v. infusion of topotecan. $^*P < 0.05$, two-tailed t test, $n = 4$ per group. **f**, Schematic depicting schedule for i.t. delivery of topotecan (50 nmol day^{-1} for 10 of 14 days) and endpoints (arrows) immediately, 4 weeks and 12 weeks after cessation of drug. **g**, **h**, Topotecan (i.t.) increased the number of UBE3A–YFP-positive spinal neurons compared to vehicle, and the unsilencing of *Ube3a–YFP* was maintained for at least 12 weeks. $^*P < 0.001$, one-way ANOVA with Bonferroni post hoc test, $n = 7$–8 per group.

In conclusion, we found that topoisomerase inhibitors can unsilence the paternal allele of *Ube3a* and that the paternally-derived protein is functional. These findings suggest that topoisomerase inhibitors have the potential to rescue the molecular, cellular and behavioural deficits associated with loss of UBE3A[7,13,28]. *Ube3a* expression is modestly upregulated in the brain of *Top2b* knockout mice[29], providing genetic support that topoisomerases regulate *Ube3a* expression. We also found that topotecan reduced expression of paternal *Snrpn* and *Ipw*, a genomic region whose deletion is associated with Prader–Willi syndrome[7,17]. To what extent topotecan regulates expression of other genes in the brain, including *Igf2r*-, *Kcnq1*- and *Gnas*-imprinted gene clusters, and whether long-term treatments with topoisomerase inhibitors produce a Prader–Willi-like condition are unknown. However, topotecan and irinotecan are approved for use in patients with cancer, penetrate into the central nervous system, and are well-tolerated when administered chronically to both adult and paediatric patients[27,30]. As well, patients treated with topoisomerase inhibitors do not display symptoms associated with Prader–Willi syndrome. Ultimately, our study indicates that topoisomerase inhibitors regulate gene expression through a transcriptional mechanism and could be used to treat symptoms associated with Angelman syndrome.

METHODS SUMMARY

All animal procedures were approved by the University of North Carolina at Chapel Hill Animal Care and Use Committee. We used male and female *Ube3a–YFP* knock-in mice[15], *Ube3a*$^{m-/p+}$ mice[13] and their age-matched, wild-type controls. High-content screening was performed on a BD Pathway 855 system. UBE3A–YFP was detected for drug screening with an anti-GFP antibody (Novus Biologicals, NB600-308; 1:1,000) because intrinsic YFP fluorescence levels were low in cultured neurons and tissue sections. All data are presented as mean $\pm$ s.e.m., with sample sizes (n) shown in figures or stated in the text. Statistical analyses were performed using SigmaPlot 11 (Systat Software). Normality tests (Shapiro–Wilk) and equal variance tests were run and passed ($P > 0.05$) before parametric statistical analyses were run.

Full Methods and any associated references are available in the online version of the paper at www.nature.com/nature.

Received 28 June; accepted 22 November 2011.
Published online 21 December 2011.

1. Kishino, T., Lalande, M. & Wagstaff, J. UBE3A/E6-AP mutations cause Angelman syndrome. *Nature Genet.* **15,** 70–73 (1997).
2. Matsuura, T. *et al. De novo* truncating mutations in E6-AP ubiquitin-protein ligase gene (*UBE3A*) in Angelman syndrome. *Nature Genet.* **15,** 74–77 (1997).
3. Sutcliffe, J. S. *et al.* The E6-Ap ubiquitin-protein ligase (*UBE3A*) gene is localized within a narrowed Angelman syndrome critical region. *Genome Res.* **7,** 368–377 (1997).
4. Albrecht, U. *et al.* Imprinted expression of the murine Angelman syndrome gene, *Ube3a*, in hippocampal and Purkinje neurons. *Nature Genet.* **17,** 75–78 (1997).
5. Rougeulle, C., Glatt, H. & Lalande, M. The Angelman syndrome candidate gene, *UBE3A/E6-AP*, is imprinted in brain. *Nature Genet.* **17,** 14–15 (1997).
6. Vu, T. H. & Hoffman, A. R. Imprinting of the Angelman syndrome gene, *UBE3A*, is restricted to brain. *Nature Genet.* **17,** 12–13 (1997).
7. Mabb, A. M., Judson, M. C., Zylka, M. J. & Philpot, B. D. Angelman syndrome: insights into genomic imprinting and neurodevelopmental phenotypes. *Trends Neurosci.* **34,** 293–303 (2011).
8. Peters, S. U. *et al.* Double-blind therapeutic trial in Angelman syndrome using betaine and folic acid. *Am. J. Med. Genet.* **152A,** 1994–2001 (2010).
9. Chamberlain, S. J. & Brannan, C. I. The Prader–Willi syndrome imprinting center activates the paternally expressed murine *Ube3a* antisense transcript but represses paternal *Ube3a*. *Genomics* **73,** 316–322 (2001).
10. Landers, M. *et al.* Regulation of the large (approximately 1000 kb) imprinted murine *Ube3a* antisense transcript by alternative exons upstream of *Snurf/Snrpn*. *Nucleic Acids Res.* **32,** 3480–3492 (2004).
11. Numata, K., Kohama, C., Abe, K. & Kiyosawa, H. Highly parallel SNP genotyping reveals high-resolution landscape of mono-allelic *Ube3a* expression associated with locus-wide antisense transcription. *Nucleic Acids Res.* **39,** 2649–2657 (2011).
12. Nakatani, J. *et al.* Abnormal behavior in a chromosome-engineered mouse model for human 15q11-13 duplication seen in autism. *Cell* **137,** 1235–1246 (2009).
13. Jiang, Y. H. *et al.* Mutation of the Angelman ubiquitin ligase in mice causes increased cytoplasmic p53 and deficits of contextual learning and long-term potentiation. *Neuron* **21,** 799–811 (1998).
14. Miura, K. *et al.* Neurobehavioral and electroencephalographic abnormalities in *Ube3a* maternal-deficient mice. *Neurobiol. Dis.* **9,** 149–159 (2002).
15. Dindot, S. V., Antalffy, B. A., Bhattacharjee, M. B. & Beaudet, A. L. The Angelman syndrome ubiquitin ligase localizes to the synapse and nucleus, and maternal deficiency results in abnormal dendritic spine morphology. *Hum. Mol. Genet.* **17,** 111–118 (2008).
16. Rougeulle, C., Cardoso, C., Fontes, M., Colleaux, L. & Lalande, M. An imprinted antisense RNA overlaps UBE3A and a second maternally expressed transcript. *Nature Genet.* **19,** 15–16 (1998).
17. Runte, M. *et al.* The IC-*SNURF–SNRPN* transcript serves as a host for multiple small nucleolar RNA species and as an antisense RNA for *UBE3A*. *Hum. Mol. Genet.* **10,** 2687–2700 (2001).
18. Watanabe, Y. *et al.* Genome-wide analysis of expression modes and DNA methylation status at sense-antisense transcript loci in mouse. *Genomics* **96,** 333–341 (2010).
19. Pommier, Y. Topoisomerase I inhibitors: camptothecins and beyond. *Nature Rev. Cancer* **6,** 789–802 (2006).
20. Hertzberg, R. P. *et al.* Modification of the hydroxy lactone ring of camptothecin: inhibition of mammalian topoisomerase I and biological activity. *J. Med. Chem.* **32,** 715–720 (1989).
21. Plaschkes, I., Silverman, F. W. & Priel, E. DNA topoisomerase I in the mouse central nervous system: age and sex dependence. *J. Comp. Neurol.* **493,** 357–369 (2005).
22. Scheffner, M., Nuber, U. & Huibregtse, J. M. Protein ubiquitination involving an E1–E2–E3 enzyme ubiquitin thioester cascade. *Nature* **373,** 81–83 (1995).
23. Beaudenon, S., Dastur, A. & Huibregtse, J. M. Expression and assay of HECT domain ligases. *Methods Enzymol.* **398,** 112–125 (2005).
24. Kumar, S., Kao, W. H. & Howley, P. M. Physical interaction between specific E2 and Hect E3 enzymes determines functional cooperativity. *J. Biol. Chem.* **272,** 13548–13554 (1997).
25. Bressler, J. *et al.* The SNRPN promoter is not required for genomic imprinting of the Prader-Willi/Angelman domain in mice. *Nature Genet.* **28,** 232–240 (2001).
26. Reik, W. Stability and flexibility of epigenetic gene regulation in mammalian development. *Nature* **447,** 425–432 (2007).
27. Gammon, D. C. *et al.* Intrathecal topotecan in adult patients with neoplastic meningitis. *Am. J. Health Syst. Pharm.* **63,** 2083–2086 (2006).
28. Greer, P. L. *et al.* The Angelman syndrome protein Ube3A regulates synapse development by ubiquitinating arc. *Cell* **140,** 704–716 (2010).
29. Lyu, Y. L. *et al.* Role of topoisomerase IIβ in the expression of developmentally regulated genes. *Mol. Cell. Biol.* **26,** 7929–7941 (2006).
30. Bomgaars, L., Berg, S. L. & Blaney, S. M. The development of camptothecin analogs in childhood cancers. *Oncologist* **6,** 506–516 (2001).

Supplementary Information is linked to the online version of the paper at www.nature.com/nature.

Acknowledgements We thank A. Beaudet and Y.-h. Jiang for providing *Ube3a–YFP* and *Ube3a*$^{m-/p+}$ mice; T. Riday and J. E. Han for assistance in i.c.v. mini-osmotic pump infusion; A. Burns for assistance in maintaining mouse colonies; V. Gukassyan for help with the Surveyor and confocal imaging systems; K. McNaughton for help with tissue sectioning; W. Zamboni for providing belotecan, rubitecan and silatecan; and W. Janzen and the Center of Integrative Chemical Biology and Drug Discovery for providing the epigenetic library. B.D.P., M.J.Z. and B.L.R. were supported by the Simons Foundation Autism Research Initiative (SFARI) and by the Angelman Syndrome Foundation. B.D.P. and M.J.Z. were supported by the National Institute of Mental Health (NIMH) (R01MH093372). B.D.P. was supported by the National Eye Institute (R01EY018323) and NC TraCS (50KR41016). M.J.Z. was supported by the National Institute of Neurological Disorders and Stroke (NINDS) (R01NS060725, R01NS067688). B.L.R. was supported by national Institutes of Health (NIH) HHSN-271-2008-00025-C, the NIMH Psychoactive Drug Screening Program, the Michael Hooker Distinguished Chair of Pharmacology, and grants from NIMH and the National Institute on Drug Abuse (NIDA). H.-S.H. was supported by a NARSAD grant from the Brain and Behavior Research Foundation Young Investigator Award and NC TraCS (10KR20910). J.A.A. was supported by NIH T32HD040127-07, the University of North Carolina-Carolina Institute for Developmental Disabilities, and an Autism Concept Award AR093464 from the US Department of Defense. A.M.M. was supported by a National Research Service Award from NINDS (5F32NS067712). I.F.K. was supported by a Joseph E. Wagstaff Postdoctoral Research Fellowship from the Angelman Syndrome Foundation. Assay development costs were partially supported by NINDS (5P30NS045892). Confocal and montage imaging was performed at the University of North Carolina at Chapel Hill Confocal and Multiphoton Imaging Facility, which is co-funded by grants from NINDS (5P30NS045892) and the National Institute of Child Health and Human Development (NICHD) (P30HD03110).

Author Contributions H.-S.H., J.A.A., A.M.M., I.F.K., M.J.Z., B.L.R. and B.D.P. conceived and designed experiments, and wrote the manuscript. All authors reviewed and edited the manuscript. H.-S.H., J.A.A., J.M. and H.-M.L. performed drug screens and validations. H.-S.H., B.T.-B., J.M. and J.W.D. performed *in vivo* studies and immunofluorescence. H.-S.H. and A.S.B. performed pharmacokinetic analyses. A.M.M. performed tests of UBE3A functionality. I.F.K. performed quantitative PCR with reverse transcription and methylation analyses. N.S. oversaw high content screening instrumentation and implemented image processing algorithms. X.C. and J.J. synthesized the lactam E ring inactive camptothecin analogue and the three indenoisoquinoline derivatives. The laboratories of M.J.Z., B.L.R. and B.D.P. contributed equally to this work.

Author Information Reprints and permissions information is available at www.nature.com/reprints. The authors declare no competing financial interests. Readers are welcome to comment on the online version of this article at www.nature.com/nature. Correspondence and requests for materials should be addressed to M.J.Z. (zylka@med.unc.edu), B.L.R. (bryan_roth@med.unc.edu) or B.D.P. (bphilpot@med.unc.edu).

METHODS

Mice. *Ube3a–YFP* mice were generated and provided by the laboratory of A. Beaudet[15]. *Ube3a*-deficient mice were generated in the laboratory of A. Beaudet[13] and backcrossed by Y.-h. Jiang onto a C57BL/6J background. C57BL/6 mice (Charles River Laboratories) were used for matings with *Ube3a–YFP*. C57BL/6J mice (Jackson Laboratories) were used for matings with *Ube3a*-deficient mice and CAST/EiJ mice (Jackson Laboratories).

Primary neuron cultures. Embryonic day 13.5 (E13.5) to E16.5 mouse cortices were dissected and trypsinized with TrypLE express at 37 °C for 10 min. Dissociated neurons were seeded onto 384-well plates coated with poly-D-lysine (0.1 mg ml^{-1}) at a density of 2×10^4 cells per well (or at a density of 1.8×10^6 cells per well for six-well plates). Neurons were cultured with Neurobasal medium with 5% fetal bovine serum, GlutaMAX (Invitrogen, catalogue no. 35050-061), B27 (Invitrogen, catalogue no. 17504-044) and Antibiotic-Antimycotic (Invitrogen, catalogue no. 15240-062) and changed into Neurobasal medium supplemented with 4.84 μg ml^{-1} uridine 5′-triphosphate (Sigma, U6625), 2.46 μg ml^{-1} 5-fluoro-2′-deoxyuridine (Sigma, F0503), GlutaMAX (Invitrogen, catalogue no. 35050-061), B27 (Invitrogen, catalogue no. 17504-044), and Antibiotic-Antimycotic (Invitrogen, catalogue no. 15240-062) at DIV1 and DIV5.

Drug libraries and compounds. Several drug libraries were used for the screening campaign including the NIMH X-901 Library (source: National Institutes of Health Chemical Synthesis and Drug Supply Program), the NIH Clinical Collection (source: National Institutes of Health), the Prestwick Library (source: Prestwick Chemical), an internal Roth laboratory library comprised mainly of central nervous system active small molecules (source: National Institute of Mental Health Psychoactive Drug Screening Program), a small molecule library of DNA methyltransferase inhibitors, protein lysine methyltransferase inhibitors and other small-molecule modulators of epigenetic targets (source: Center for Integrative Chemical Biology and Drug Discovery, UNC-CH). Suberoylanilide hydroxamic acid (SAHA) was purchased from Cayman Chemical. Irinotecan, zebularine, hydralazine, procainamide, 5-aza-2′-deoxycytidine (decitabine), etoposide, tenoposide, amsacrine and ICRF-193 were all obtained from Sigma-Aldrich. Topotecan, camptothecin (CPT), 10-hydroxy-CPT, 7-ethyl-CPT and 7-ethyl-10-hydroxy-CPT (SN38) were obtained from MOLCAN Corporation. ICRF-187 was provided by the National Cancer Institute's Developmental Therapeutics Program. Belotecan, silatecan and rubitecan were provided by W. Zamboni (University of North Carolina Eshelman School of Pharmacy). The indenoisoquinoline derivatives NSC706744, NSC725776 and NSC724998 were synthesized as described[31,32]. The inactive lactam E ring-CPT analogue was synthesized as described[20].

High-content screening microscopy and small-molecule screening. Primary cortical neurons were isolated from E13.5-16.5 *Ube3a–YFP* mice. Screening was performed in quadruplicate at DIV7 using multiple chemical libraries and a compound concentration of 10 μM in 0.2% DMSO vehicle. After 72 h of drug exposure, neurons were fixed with 4% paraformaldehyde in PBS for 35 min, permeabilized with 0.3% Triton X-100 in PBS on ice for 30 min, and blocked by 5% goat serum with 0.1% Triton X-100 in PBS at room temperature for 1 h. Cells were incubated with a rabbit polyclonal antibody to GFP (1:1,000, Novus Biologicals, NB600-308) at room temperature for 1 h and then incubated with Alexa Fluor 488 goat antibody to rabbit IgG (1:200, Invitrogen, A11008) and DAPI (1:10,000, Invitrogen, D-1306) at room temperature for 30 min. Individual wells of immunofluorescence-processed plates were imaged for DAPI or Alexa 488 fluorescence using the BD Pathway 855 high-content imaging microscope with a 488-nm excitation/515-nm long-pass filter. Antibody-enhanced UBE3A–YFP fluorescence intensities were determined from individual neurons in drug-treated wells and normalized to neurons in wells treated with 0.2% DMSO (vehicle control). Analyses were performed with custom macros and algorithms using NIH Image J and Arrayscan Cell Profiler software programs (Thermo Scientific/Cellomics). These image analyses enabled masking of nuclei in individual neurons and determination of UBE3A–YFP fluorescence intensities in the nuclei of individual neurons (see Supplementary Fig. 1). Drug-induced increases of >50% were initially binned as screening 'hits' if (1) the increases were consistently observed across replicate wells and (2) no apparent toxicities were observed by assessing nuclear structure of neurons co-stained with DAPI. Effective 'hit' compounds were validated in formal dose–response experiments to determine relative compound potencies (EC_{50}) and efficacies (E_{max}).

After the initial identification of irinotecan as an active, other topoisomerase inhibitors were screened. DIV7 primary neurons from *Ube3a*$^{m+/pYFP}$ *mice* were dose-treated for 72 h with topoisomerase I and II inhibitors in ten point dose–responses in full- and half-log molar concentrations (1 nM to 30 μM). Neurons were fixed, processed for immunofluorescence, and UBE3A–YFP fluorescence intensities were again determined by high-content imaging microscopy. The dose–response results were analysed by least squares sigmoidal dose–response curve-fitting models using Graphpad Prism 5.0 (Graphpad Software). The calculated EC_{50} values (potencies) and *Y*-value top plateau (estimated efficacies or E_{max}) enabled comparative analyses of the relative potency and efficacy of the identified compounds. To control for potential false positive 'hit' compounds, cortical neurons from wild-type mice, which lack *Ube3a–YFP*, were also treated to determine if 'hit' compounds exhibit inherent fluorescence.

A *Z′*-factor score was determined to assess the appropriateness of the screening platform by comparing UBE3A–YFP maternal and paternal fluorescence signals at DIV10. This was done by determining the mean cellular UBE3A–YFP fluorescence of >1,200 neurons in quadruplicate wells for both genotypes, which were normalized to age-matched vehicle-treated control wells. The score was calculated using the following formula: Z' factor $= 1 - ((3 \times (\text{s.d. maternal UBE3A–YFP} + \text{s.d. paternal UBE3A–YFP}))/(\text{mean maternal UBE3A–YFP} - \text{mean paternal UBE3A–YFP})$.

Immunofluorescence staining in central nervous system tissues. For immunocytochemistry in brain tissues, mice were perfused with 4% paraformaldehyde in 0.1 M PBS, post-fixed overnight, and cryoprotected with 20% sucrose in 0.1 M phosphate buffer, pH 7.4 for two days. Sections (60 μm) were collected and permeabilized with 0.3% Triton X-100 in 0.1 M phosphate buffer for 30 min, and blocked by 5% goat serum for 1 h. Sections were incubated with rabbit polyclonal antibody to GFP (1:1,000, Novus Biologicals, NB600-308) at 4 °C overnight and then incubated with Alexa Fluor 488 goat antibody to rabbit IgG and DAPI for 2 h at room temperature. Images were acquired using a Zeiss LSM 510 and 710 confocal microscopes.

For immunocytochemistry in spinal cord, lumbosacral spinal cord (approximately L1 to S2 and inclusive of the area corresponding to intrathecal injection site) was removed from each mouse and immersion-fixed for 8 h in cold 4% paraformaldehyde and 0.1 M phosphate buffer (pH 7.4). After a period of cryoprotection in 30% sucrose in 0.1 M phosphate buffer, each spinal cord was sectioned on a cryostat at 40 μm. Sections to be stained immediately were collected in PBS, sections to be saved for future study were placed in a PBS/ethylene glycol/glycerol solution and stored at −20 °C. Every fourth section was incubated overnight in a mixture containing a chicken IgY to GFP (1:750; Aves Labs, GFP-1020) and a mouse IgG_1 to NeuN (1:250; Millipore, MAB377) and treated the following day with a cocktail containing goat anti-chicken IgY-Alexa 488 (1:200; Invitrogen, A-11039), goat anti-mouse IgG1-Alexa 568 (1:200; Invitrogen, A-21124) and DRAQ5 (1:10,000; Axxora, BOS-889-001). Immunostained sections were mounted from PBS onto SuperFrost Plus Slides (Fisher), which were then air-dried briefly, rehydrated with PBS, and coverslipped with FluoroGel (Electron Microscopy Sciences). For quantification studies, sections were imaged using a Nikon Eclipse 80i with Surveyor mosaic imaging software. For qualitative assessment, sections were imaged as maximal projections on a Zeiss LSM 510.

Optical intensity measurement of UBE3A–YFP in brain tissue and cell counting of UBE3A–YFP-positive neurons in spinal cord. For optical intensity measurement in selected brain regions, sections were imaged using a Zeiss LSM 510 confocal microscope. With custom macros created using ImageJ software[33], optical intensity of UBE3A–YFP was measured in different regions of hippocampus and striatum from vehicle- and topotecan-treated mice. Image intensity levels were normalized to background intensities from appropriate regions in vehicle-treated mice. Brain sections between Bregma −1.22 mm and −2.06 mm were chosen for analysis ($n = 5$ sections per mouse for hippocampus and $n = 3$–5 sections per mouse for striatum).

For cell counting in spinal cord, we analysed 14 to 18 sections per mouse in segments corresponding to the injection site. Slices were imaged using a Nikon Eclipse 80i microscope equipped with a Qimaging Retiga Exi high-speed CCD camera system and Surveyor mosaic imaging software using a ×10 objective. For qualitative purposes, we also imaged selected sections on a Zeiss LSM 510 confocal microscope. Cells were counted manually by individuals blind to the experimental groups from raw (unprocessed) images using ImageJ and Cellprofiler[34] software.

YFP intensity levels from confocal *XYZ* image stacks were measured using a semi-automated macro with ImageJ. Individual YFP-positive cells were selected by eye, the criteria being the *Z* plane having the largest area for each cell. Cell regions were defined by intensity thresholding or manual tracing and the average YFP intensity and percent saturation were calculated for each cell.

Western blotting. E13.5–E15.5 primary cortical neurons from *Ube3a–YFP*, *Ube3a*-deficient or wild-type mice were plated in six-well plates. At DIV7, neurons were treated with drug or 0.1% DMSO for 72 h, and then total protein lysates were obtained by lysis buffer (1% Triton X-100, 5 mM EDTA, 0.15 M NaCl, 10 mM Tris-HCl, pH 7.5, phosphatase inhibitor cocktails 1, protease inhibitor cocktail). To assess UBE3A–YFP or UBE3A protein levels, 7.5 μg of total protein lysates from *Ube3a–YFP* or *Ube3a*-deficient neurons were separated by 8% SDS-polyacrylamide gel electrophoresis. Proteins were then transferred to nitrocellulose membranes, and immunoblotting was performed using a rabbit anti-GFP antibody (Novus,

1:500) and Alexa Fluor 680 goat anti-rabbit IgG (Invitrogen, 1:5,000) or rabbit anti-UBE3A antibody (Abcam, 1:500) and Alexa Fluor 680 goat anti-rabbit IgG (Invitrogen, 1:5,000). UBE3A–YFP or native UBE3A protein bands were visualized using an Odyssey system (LI-COR Biosciences). To control for protein loading, UBE3A–YFP or UBE3A protein levels were normalized to actin levels detected in each sample.

Ubiquitin thioester assay. DIV10 cortical neurons were collected and lysed in immunoprecipitation buffer (20 mM Tris-HCl, 3 mM EDTA, 3 mM EGTA, 150 mM NaCl, 1% Triton X-100, pH 7.4) containing 10 mM sodium fluoride, 1.0 mM sodium orthovanadate, 1.0 μg ml^{-1} aprotinin, and 0.1 mM DTT. UBE3A protein was immunoprecipitated from cell extracts with 5.0 μg of an anti-UBE3A antibody (Bethyl Laboratories) overnight at 4 °C and then washed twice with immunoprecipitation buffer containing 500 mM NaCl, followed by ubiquitin buffer (50 mM Tris, 5 mM $MgCl_2$, pH 7.6). For *in vitro* ubiquitination of immunoprecipitated UBE3A, UBE3A was mixed with 0.1 μg E1, 0.5 μg UBCH7, 2.5 μg ubiquitin (Boston Biochem) and 10 mM ATP in a total reaction volume of 20 μl. The reaction was incubated at room temperature for 10 min and end products were stopped in 2× SDS sample buffer with or without DTT. Samples were boiled, separated by SDS–PAGE gel electrophoresis, transferred to PVDF membrane, and immunoblotted with an anti-UBE3A or anti-ubiquitin (Santa Cruz) antibody.

Topoisomerase depletion assay. DIV7 cortical neurons were treated with 300 nM topotecan or vehicle for 72 h. Cells were collected and lysed on ice for 30 min in RIPA buffer (50 mM Tris-HCl, 150 mM NaCl, 1% Triton X-100, 0.5% sodium deoxycholate, 0.1% SDS, pH 7.4) to preserve topoisomerase cleavable complexes. Cell extracts were then centrifuged at 14,000 r.p.m. at 4 °C to pellet insoluble debris. 30 μg of the cell supernatant was diluted in 2× SDS sample buffer and separated on a 7.5% SDS–PAGE gel, transferred to nitro cellulose membrane, and immunoblotted with an anti-topoisomerase I antibody (Santa Cruz) to detect free topoisomerase I. An anti-β-tubulin (Sigma) antibody was used as a loading control.

Quantitative PCR. For quantitative reverse transcriptase polymerase chain reaction (qRT–PCR) analysis, total RNA was extracted from cortical cultures treated with 300 nM topotecan using TRIzol reagent (Invitrogen). First strand cDNA synthesis was performed on 500 ng–2 μg total RNA using Superscript III reverse transcriptase (Invitrogen) primed with random hexamers. qPCR reactions used SYBR green (Invitrogen) and were run on a Rotorgene 3000 (Corbett Research). Standard curves and C_t values were generated using Rotorgene analysis software version 6.0. Expression of *Ube3a*, *Ube3a–ATS (2)*, *Ube3a-ATS (3) (Ipw)* and *Snrpn* were determined after normalization of each complementary DNA sample to expression levels of the housekeeping genes *Rpl22* and *Actb*. Primers were as follows: *Ube3a* F (5′-CAAAAGGTGCATCTAACAACTCA-3′), *Ube3a* R (5′-GGGGAATAATCC TCACTCTCTC-3′), *Snrpn* 1-3 F (5′-TTGGTTCTGAGGAGTGATTTGC-3′)[35], *Snrpn* 3 R (5′-CCTTGAATTCCACCACCTTG-3′)[35], *Ipw* B/C F (5′-TCACC ACAACACTGGACAAAA-3′)[10], *Ipw* B/C R (5′-TCACCACAACACTGGACAA AA-3′)[10], *Ube3a–ATS* F (5′-GGCACCCTTGTTTGAAACTT-3′), *Ube3a–ATS* R (5′-GCTCATGACCCTGTCCTTTC-3′), *Rpl22* F (5′- AAGAAGCAGGTTTTGA AG-3′), *Rpl22* R (5′-TGAAGTGACAGTGATCTTG-3′), *Actb* F (5′- CAGCTT CTTTGCAGCTCCTT-3′), *Actb* R (5′- CACGATGGAGGGGAATACAG-3′).

Bisulphite sequencing. Genomic DNA was extracted from C57BL/6 (female) × CAST/EiJ (male) F1 hybrid cortical cultures treated with 300 nM topotecan using TRIzol reagent. Bisulphite conversion was performed on 200 ng genomic DNA using a MethylCode kit (Invitrogen). Converted DNA (1 μl) was used as template for PCR. A first round of PCR was performed as described in ref. 36 using the W18 and W19 or W16 and W17 primer sets[36]. A second semi-nested round of PCR was performed using 1 μl of the primary PCR reaction as template. For semi-nested PCR, the W18 primer was used with the nested W19-inside primer (5′-AAATAAAATACACTTTCACTACTAAAATC-3′), or the W16 primer was used with the nested W17-inside primer (5′-ACAACAAAACTTCTATCCACAC-3′). Products were separated on an agarose gel and extracted using the QIAquick gel extraction kit (Qiagen). Purified DNA was ligated into the pGem-T Easy vector (Promega). Individual clones were amplified and sequenced to assess methylation status and parent of origin.

Intrathecal injection. Topotecan (50 nmol in 5 μl, unless noted) was injected into unanaesthetized mice via a 30-gauge needle attached to a 50 μl Luer-hub Hamilton syringe using the direct lumbar puncture method[37]; injections were made at lower lumbar levels. Following the injection, the syringe is rotated slightly and removed. Topotecan was dissolved with 50 mM tartrate acid buffer in 0.9% saline. Comparable vehicle injections were made in control mice.

Intracerebroventricular drug infusions. Mice with paternal *Ube3a–YFP* (*Ube3a*$^{m+/pYFP}$) were anesthetized with ketamine/xylazine (120 mg per kg; 9 mg per kg) and positioned in a stereotaxic apparatus. The scalp was shaved and cut, and the skull exposed. The local anaesthetic (bupivacaine, 2.5 mg ml^{-1}) was applied to the skull, and mineral oil was applied to protect the eyes of the mice. Acetone was applied on the skull to remove any lipid tissues on the skull as well as to dry the skull surface for optimal adhesion. Next, a cannula (Brain Infusion Kit 1, DURECT Corporation) was positioned into a lateral ventricle at the following coordinates (−0.3 mm A/P, +1.0 mm M/L, −2.5 mm D/V), as described[38]. The free end of the cannula was connected to a mini-osmotic pump (Alzet, Model 2001 or 2002) via a 2.5-cm piece of polyethylene (PE) tubing (DURECT Corporation). The mini-osmotic pump and the connecting PE tubing were filled with, respectively for Alzet models 2002 and 2001, 16.34 mM or 47.17 mM topotecan (CPT06, Molcan Corporation) dissolved in 50 mM tartaric acid with 0.9% saline, unless indicated. The filled pumps were incubated in sterile saline at 37 °C for at least 4 h before being implanted under the dorsal skin of the mouse's back. The cannula base and the attached piece of PE tubing were fixed to the skull with Loctite cyanoacrylic 454. The incision site was closed with prolene suture. During and after surgery, mice were placed on a heating pad to maintain body temperature. 14 days (Alzet model 2002) or five days (Alzet model 2001) following minipump implantation, mice were killed following pentobarbital overdose (150 mg per kg, intraperitoneally) and brains were removed for immunofluorescence staining or pharmacokinetic analysis.

Pharmacokinetic analysis of topotecan. Total topotecan concentrations in blood and brain homogenate were determined by liquid chromatography/triple quadrupole mass spectrometry (HPLC/MS-MS). The HPLC-MS/MS system consisted of two Shimadzu Scientific solvent delivery pumps, a Valco switching valve, a thermostated (6 °C) LEAP HTC autosampler, and an Applied Biosystems API3000 triple quadrupole mass spectrometer. Reversed-phase gradient chromatography was used to elute the compounds from an Aquasil (C18 3 μm, 50 × 2.1 mm) analytical column at a flow rate of 0.3 ml min^{-1}, following a 10 μl injection. Starting conditions for each injection was 85% aqueous (0.1% v/v formic acid in water) and 15% organic (0.1% v/v formic acid in methanol). This was held constant for 0.7 min. After 0.7 min, the organic phase increased linearly to 95% 4.5 min post-injection. The solvent composition was held at 95% organic for 0.5 min to wash the column. The column was re-equilibrated to starting conditions for the final 1 min. Total run time was 6 min. Eluent was diverted to waste for the first 1.5 min. After 1.5 min post-injection, 100% of the eluent was directed to the mass spectrometer. The mass spectrometer was connected to the HPLC system by a TurboIonSpray interface. User-controlled voltages, gas pressures and source temperature were optimized via direct infusion of topotecan, *d*6-topotecan (internal standard) and irinotecan (internal standard). All were analysed in positive ion mode using the following transitions preset in multiple reaction monitoring scans: topotecan 422.0→377.1, *d*6-topotecan (428.0→377.1) and irinotecan 587.2→587.2 (parent to parent transition). To eliminate instrument error due to either in source fragmentation or to cross-talk, care was taken to ensure analytical separation between topotecan and its desmethyl metabolite. Automated sample acquisition and data analysis was performed using the Analyst software (version 1.4.1, Applied Biosystems, Foster City, CA). Calibration curves, prepared from standards prepared in duplicate using appropriate matrix, were generated based on peak area ratios (analyte:internal standard) and followed a linear fit with $1/x^2$ weighting. The lower limit of topotecan quantification (LLQ) was 0.01 μM in both blood and brain homogenate (0.03 ng per mg of brain). Unknown brain and brain homogenate samples and spiked matrix standards were analysed following addition of internal standard and protein precipitation using 4× volume of methanol-containing formic acid (0.1% v/v). Note that brain homogenates were taken from entire hemispheres; because our homogenates included the ventricular cerebrospinal fluid where drug is likely to accumulate, our drug concentrations likely overestimate the concentrations in parenchymal brain tissue.

31. Cushman, M. *et al.* Synthesis of new indeno[1,2-*c*]isoquinolines: cytotoxic non-camptothecin topoisomerase I inhibitors. *J. Med. Chem.* **43,** 3688–3698 (2000).
32. Nagarajan, M. *et al.* Synthesis and evaluation of indenoisoquinoline topoisomerase I inhibitors substituted with nitrogen heterocycles. *J. Med. Chem.* **49,** 6283–6289 (2006).
33. Abramoff, M. D., Magelhaes, P. J. & Ram, S. J. Image processing with ImageJ. *Biophotonics International* **11,** 36–42 (2004).
34. Lamprecht, M. R., Sabatini, D. M. & Carpenter, A. E. CellProfiler: free, versatile software for automated biological image analysis. *Biotechniques* **42,** 71–75 (2007).
35. Tsai, T. F., Jiang, Y. H., Bressler, J., Armstrong, D. & Beaudet, A. L. Paternal deletion from Snrpn to Ube3a in the mouse causes hypotonia, growth retardation and partial lethality and provides evidence for a gene contributing to Prader-Willi syndrome. *Hum. Mol. Genet.* **8,** 1357–1364 (1999).
36. Peery, E. G., Elmore, M. D., Resnick, J. L., Brannan, C. I. & Johnstone, K. A. A targeted deletion upstream of *Snrpn* does not result in an imprinting defect. *Mamm. Genome* **18,** 255–262 (2007).
37. Fairbanks, C. A. Spinal delivery of analgesics in experimental models of pain and analgesia. *Adv. Drug Deliv. Rev.* **55,** 1007–1041 (2003).
38. Pierce, A. A. & Xu, A. W. De novo neurogenesis in adult hypothalamus as a compensatory mechanism to regulate energy balance. *J. Neurosci.* **30,** 723–730 (2010).